Computational Modelling of the Neuromuscular Junction in Myasthenia Gravis

Yasmine Mahmoud, Nada Khaled, Mina Raafat, Mina Wagdy, Kirellos Safwat, Enjy Ashraf, and Shahd Ahmed
Department of Systems and Biomedical Engineering, Faculty of Engineering, Cairo University

***Abstract*— This research paper presents a computational model that investigates the reaction-diffusion mechanisms of acetylcholine in the synaptic cleft of the neuromuscular junction (NMJ). The model utilizes the Finite Element Method, a stable numerical approach to simulate the dynamics of acetylcholine release in normal synaptic physiology compared to Myasthenia Gravis (MG). By examining the impact of diffusion parameters and NMJ geometry and describing the dynamics of acetylcholine and receptors in the presence of activated enzymes, the model enhances our understanding of neuromuscular disorders. The simulation outcomes align with the physiological explanation, making this model a valuable tool for in-depth visualization of NMJ dynamics.**

Keywords—Neuromuscular, Junction, Myasthenia, Gravis, PDE, Modelling, MATLAB, Acetylcholine, Diffusion

I. Introduction and problem definition

The neuromuscular junction (NMJ) is a critical synapse connecting motor neurons and skeletal muscle cells. Motor neurons release acetylcholine, a neurotransmitter, into the synaptic cleft, initiating muscle contraction by binding to receptors on muscle fibers. NMJ degeneration, caused by factors like injury and aging, leads to conditions such as Myasthenia Gravis (MG), where the immune system produces antibodies that block receptor sites, resulting in symptoms like drooping eyelids and muscle weakness.

The NMJ's intricate three-dimensional structure poses a challenge for traditional analytical methods, making mathematical models crucial for understanding its dynamics. These models primarily focus on acetylcholine diffusion within the NMJ, essential for nerve-to-muscle signal transmission.

A few epidemiological studies on the prevalence of neuromuscular disorders have been undertaken in Egypt in Qena governorate. Out of 9303 participants, 448 cases were reported positive. [4]

TABLE I. Prevalence of Neuromuscular Diseases in Qena, Egypt [4]

	Definite Neuropathy	**Focal Compression Neuropathies**	**Carpal Tunnel Syndrome**
Number of Cases	408	167	155
	Bell's Palsy	**Myasthenia Gravis**	**Diabetic Neuropathy**
Number of Cases	15	2	155

TABLE II. Crude Prevalence Ratings of Neuromuscular Diseases in Qena, Egypt [4]

	Definite Neuropathy	**Focal Compression Neuropathies**	**Carpal Tunnel Syndrome**
CPR (%)	4.39%	1.8%	1.67%
	Bell's Palsy	**Myasthenia Gravis**	**Diabetic Neuropathy**
CPR (%)	0.16%	21/105	1.67%

In Qena governorate, Egypt, neuromuscular disorders show a higher prevalence in rural areas. Globally, MG prevalence varies by location, with rates ranging from 150 to 200 cases per 1,000,000 people. The United States estimates 14 to 20 cases per 100,000 people, while Europe has 56,000 to 123,000 individuals with MG. Women are more affected, with a 3:1 sex ratio before 40, but after 50, men and women show a closer 1:1 ratio. Stress, infections, pregnancy, and childbirth are linked to MG development.

MG onset varies by sex and age, with women commonly affected in their 20s and 30s, while men are diagnosed in their 70s and 80s. There is a 99.6% probability that the mean age difference at MG diagnosis between sexes exceeds 10 years. The most common age of MG onset is 20 to 40, with women constituting 60% of these cases, and nonwhite patients typically experiencing earlier onset.

Understanding these demographics and factors is crucial for advancing MG research and treatment. Treatment can be done by slowing down the breakdown of acetylcholine using anticholinesterase inhibitors such as pyridostigmine. This agent increases the number of interactions between acetylcholine and acetylcholine receptors in the neuromuscular junction. [3]

II. Literature review

A. Reviewing Process

We conducted a thorough reviewing process, starting with scanning multiple research libraries like Academia, ResearchGate, Springer, and google scholar. The initial search process yielded around 23,000 papers. After excluding all papers using other modelling approaches that are not related to PDEs the number of papers came closer to around 6,300 papers. We then proceeded to exclude all papers discussing diseases that we are not concerned about, leaving only papers concerned with modelling the NMJ in general and those discussing Myasthenia Gravis, which resulted in the number of remaining papers to be about 250 papers. From there we proceeded to exclude papers based on the relevance of their titles, abstracts, and the numerical methods used, which narrowed them down to around 20 papers, from which we selected 3 papers that we thought were most relevant to our research.

The three selected papers discussed multiple numerical methods such as: Finite Element Method (FEM), Finite Difference Method (FDM), and Spectral Element Method (SEM). They also provided valuable information about the Neuromuscular Junction from a physiological point of view. This was extremely helpful in forming a general image of its structure and deciding which method to use in the modelling stage of this research.

In 1998, Smart JL et al. [5] looked at how messages pass between nerves. Some studies have looked at how acetylcholine sticks to receptors, but not as much about how it is spread around in detailed nerve models.

They used a method called finite element to study this. It helped them model complex shapes, look at long time periods, and consider background levels of acetylcholine (ACh). They also showed clusters of acetylcholinesterase (AChE) and how many tiny containers release ACh at once. To make sure this method is accurate. They compared their results to other studies and real experiments. They also explored how different parts of the neuromuscular junction, like AChE, affect the strength and timing of the signal.

To understand this better, the authors used a simplified model and mathematical calculations. They treated acetylcholine like a spread-out substance, and used a flexible method to model its movement. Their computer simulations matched up with real experiments and other computer models. This helped them learn more about how messages pass between nerves and muscles. The model includes a detailed representation of the NMJ, including secondary folds and AChE clusters.

The simulations also demonstrate that while AChE affects the first burst of released ACh, its main function seems to be in the later phases of synaptic transmission.

In 2011, Khaliq et al. [6] introduced a comprehensive 3D model elucidating the intricate dynamics of acetylcholine and receptor interactions within the neuromuscular junction. The model, depicting a disk-shaped volume, employs a 3D diffusion equation with nonlinear reaction terms, solved through a stable numerical method with Neumann boundaries in cylindrical coordinates.

The investigation extends to exploring the sensitivity of open receptor dynamics to alterations in diffusion parameters and the volume of the neuromuscular junction. Anisotropic diffusion and non-symmetric transmitter emission at the presynaptic membrane are considered, treating the NMJ as a three-dimensional molecular transport and reaction system with defined circular planes as boundaries.

Accordingly, a diffusion-reaction equation in cylindrical coordinates describes acetylcholine diffusion, considering diffusion coefficients in radial, angular, and transverse directions within the cleft.

To solve these equations, the researchers employ a mesh structure facilitating a second-order accurate and unconditionally stable finite difference scheme. The Runge-Kutta method, specifically a fourth-order accurate scheme, ensures precise values for key terms. Notably, the mesh design maintains stability, crucial for the small length of the cleft.

The paper also showcases advances in modeling processes, discussing simulations and advancements in post-2000 research, including the finite element method. The study entertains a 3D model using an enhanced Crank-Nicolson finite difference scheme with Neumann boundary conditions. Simulations closely align with experimental measurements and previous research on open receptor dynamics, exploring the impact of diffusion parameter variations and presenting examples of asymmetric acetylcholine release.

In 2013, Liu et al. [7] developed a numerical model of high order accuracy for complex geometry to simulate the processes in an NMJ cleft.

The model provides a comprehensive description of the three-dimensional reaction and diffusion processes in the neuromuscular junction. It can accurately predict the concentration rates of acetylcholine with receptors and enzymes. The simulation results align with experimental measurements of the maximum number of open receptors during a normal action potential, and the model has the potential to facilitate further investigation into the dynamics within the NMJ.

The authors focus on studying the complex chemistry in the NMJ associated with the reaction diffusion processes in complex geometry rather than using the cylindrical coordinates method that researchers before them used, which is a lot less accurate, and investigate the underlying mechanisms using numerical methods. They compare the limitations of the finite element method (FEM), used in other research papers, with the spectral element method (SEM) and choose to use SEM due to its ability to achieve higher accuracy and resolution in simulating the NMJ system. The authors developed a 3D model that simulates the interaction of acetylcholine and acetylcholine receptors in the neuromuscular junction when the enzyme is activated.

They check the model's accuracy by matching its results with the known values of the peak number and time of open receptors during a normal action potential. The model also shows its flexibility by exploring how the receptor dynamics change with different receptor distributions, diffusion parameters, and neurotoxin exposures.

B. Reviewing Conclusion

The three papers focus on simulating and analyzing synaptic transmission in the neuromuscular junction, particularly emphasizing acetylcholine diffusion and interactions with receptors and enzymes. Smart et al. [5] employ a continuum finite element model, Khaliq et al. [6] introduce a 3D mass diffusion-reaction model, and Liu et al. [7] develop a high-accuracy numerical model using the spectral element method.

Our research aims to complement these studies by incorporating the finite element method and providing a comprehensive analysis of its applicability and advantages in studying ACh dynamics within the NMJ. This addition will contribute to a more nuanced understanding of neurotransmitter interactions and further enhance the accuracy and completeness of existing simulation models.

III. MATHEMATICAL MODELLING

All mathematical modelling is an abstract mathematical representation of reality. Most real-world issues may be explained by differential equations, particularly partial differential equations (PDEs), because of the world's dynamic nature. So, we built a PDE model on the dynamics of the neurotransmitter acetylcholine and acetylcholine

receptors within the NMJ, by delving into the diffusion and reaction processes. We studied the biochemical processes within the NMJ extensively. In simulations, a 3D mesh is used to represent the NMJ cleft.

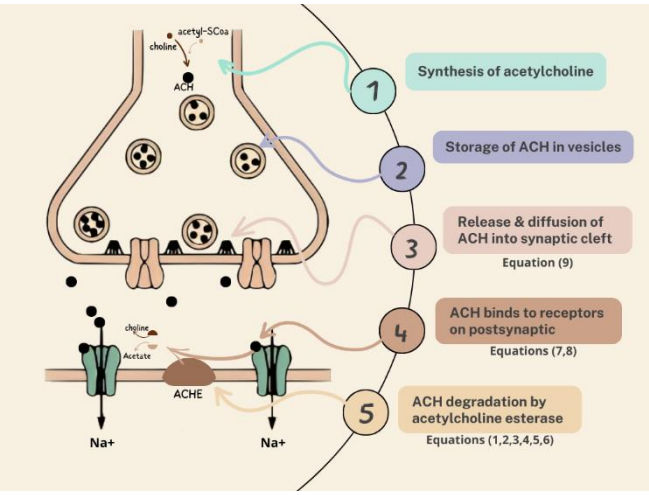

Fig. 1. Lifetime of Acetylcholine in the Neuromuscular Junction.

A. *Acetylcholine-Acetylcholinestrase Reactions*

In the governing partial differential equations (PDE) of the simulation model, we consider the following chemical reactions:

$$A + E \underset{k_{-E1}}{\overset{k_{E1}}{\rightleftharpoons}} AE \qquad (1)$$

$$AE \xrightarrow{k_{E2}} acE \qquad (2)$$

$$acE \xrightarrow{k_{E3}} E \qquad (3)$$

Equation (1) represents the reversible binding of acetylcholine (A) to acetylcholinesterase (E) to form the Michaelis ligand-substrate complex (AE). Equation (2) represents the formation of the acylate enzyme (acE) intermediate from the Michaelis ligand-substrate complex (AE). Equation (3) represents the breakdown of the acylate enzyme (acE) intermediate into acetylcholinesterase (E) and the acetylated substrate.

The reaction rates of the chemical reaction equations (1), (2), and (3) involving acetylcholinesterase enzyme, are governed by the following differential equations:

$$\frac{\partial(E)}{\partial t} = -k_{E1}(A)(E) + k_{-E1}(AE) + k_{E3}(acE) \qquad (4)$$

$$\frac{\partial(AE)}{\partial t} = k_{E1}(A)(E) - k_{-E1}(AE) - k_{E2}(AE) \qquad (5)$$

$$\frac{\partial(acE)}{\partial t} = -k_{E3}(acE) + k_{E2}(AE) \qquad (6)$$

Where k_{E1}, k_{-E1}, k_{E2}, k_{E3} are the forward and backward reaction constants for E, AE, acE, respectively.

In equation (4), $\frac{\partial(E)}{\partial t}$ represents the rate of change of the enzyme concentration (E) with respect to time. It tells us how fast the enzyme concentration is changing. k_{E1} (A)(E) accounts for the rate at which acetylcholine (A) combines with the enzyme (E) to form the complex (AE). k_{-E1} (AE) represents the rate at which the complex (AE) breaks down back into acetylcholine (A) and the enzyme (E). k_{E3} (acE) indicates the rate at which the acylate enzyme (acE) is formed from the enzyme (E).

So, in simple terms, this equation describes how the concentration of the enzyme changes over time. It decreases when acetylcholine combines with it, increases when the complex breaks down, and decreases again when acylate enzyme is formed.

In equation (5), $\frac{\partial(AE)}{\partial t}$ is the rate of change of the complex concentration (AE) over time. k_{E1} (A)(E) represents the rate at which acetylcholine (A) and enzyme (E) combine to form the complex (AE). k_{-E1} (AE) is the rate at which the complex (AE) breaks down back into acetylcholine (A) and enzyme (E). k_{E2} (AE) is the rate at which the complex (AE) turns into the acylate enzyme (acE). So, this equation describes how the concentration of the complex changes. It increases when acetylcholine and enzyme combine, decreases when the complex breaks down, and decreases again when it turns into the acylate enzyme.

As for equation (6), $\frac{\partial(acE)}{\partial t}$ represents the rate of change of the acylate enzyme concentration (acE) with respect to time. $-k_{E3}$ (acE) The rate at which the acylate enzyme (acE) breaks down. k_{E2} (AE) The rate at which the complex (AE) turns into the acylate enzyme (acE). So, this equation describes how the concentration of the acylate enzyme changes over time. It decreases when the acylate enzyme breaks down and increases when the complex turns into the acylate enzyme.

B. *Acetylcholine-Receptors Equations*

The receptor-related chemical reactions are listed as follows:

$$A + R \underset{k_{-R}}{\overset{2k_R}{\rightleftharpoons}} AR$$

$$A + AR \underset{2k_{-AR}}{\overset{k_{AR}}{\rightleftharpoons}} A_2R$$

$$A_2R \underset{k_{open}}{\overset{k_{close}}{\rightleftharpoons}} A_2R^{open} \qquad (7)$$

Equations (7) describe the binding of acetylcholine to the different types of receptors. The forward and backward reaction rates are unique to each type of receptor. If it is multiplies by two, it means that two molecules of acetylcholine can bind to or dissociate from the receptor, depending on whether it is a forward or a backward reaction. We can denote the equilibrium constant C = forward rate/backward rate. The higher the value of C, the more likely the acetylcholine will bind to the receptor. The forward reaction rate given by k_{open} means that the double bound receptor can open and allow ions to flow through. The

backward reaction rate given by k_{close}, means that the double bound receptor can close and stop the ion flow.

These reactions are governed by the following differential equations:

$$\frac{\partial(R)}{\partial t} = -2k_R(A)(R) + k_{-R}(AR)$$

$$\frac{\partial(AR)}{\partial t} = 2k_R(A)(R) - k_{-R}(AR) - k_{AR}(A)(AR) + 2k_{-AR}(A_2R)$$

$$\frac{\partial(A_2R)}{\partial t} = k_{AR}(A)(AR) - 2k_{-AR}(A_2R) - k_{open}(A_2R) + k_{close}(A_2R^{open})$$

$$\frac{\partial(A_2R^{open})}{\partial t} = k_{open}(A_2)(R) - k_{close}(A_2R^{open}) \quad (8)$$

Where $2k_R$, k_{-R}, k_{AR}, $2k_{-AR}$, k_{close}, k_{open} are the forward and backward reaction constants for R, AR, A2R, A2Ropen, respectively.

Equations (8) describe the change in concentration of the different types of receptors over time at a fixed point in space. The calculated value is the net rate of binding and unbinding of acetylcholine to the receptor. Negative terms represent the loss of receptors due to binding with acetylcholine, while positive terms represent the gain of receptors due to unbinding of acetylcholine. In the last two PDEs, the gain and loss are due to opening or closing of receptors, depending on the sign of the term and whether we are concerned with the opened or closed receptors. The second PDE also describes the transition between AR and A_2R, and the third PDE describes the transition between A_2R and A_2R^{open}. In this case, the positive term represents gain of bound receptors, and the negative term represents their loss. In the third equation, the term $-k_{open}(A_2R)$ represents the loss of (A_2R) due to opening and forming (A_2R^{open}), while the term $k_{close}(A_2R^{open})$ represents the gain of (A_2R) due to closing from (A_2R^{open}).

$$\frac{\partial(A)}{\partial t} = D_x\frac{\partial^2 A}{\partial x^2} + D_y\frac{\partial^2 A}{\partial y^2} + D_z\frac{\partial^2 A}{\partial z^2} - 2k_R(A)(R) + k_{-R}(AR) - k_{AR}(A)(AR) + 2k_{-AR}(A_2R) - k_{E1}(A)(E) + k_{-E1}(AE) \quad (9)$$

Equation (9) describes the change in concentration of acetylcholine (A) over time in a three-dimensional space, where Dx, Dy, Dz are diffusion coefficients in the x, y, z directions, respectively.

C. PDE Model

1) Assumptions

We assume acetylcholine cannot diffuse outside of the synaptic cleft. Physiologically speaking, this is not entirely true, as there are glial cells that can absorb the neurotransmitter. However, it is considered negligible compared to degradation of acetylcholine.

Breaking down of acetylcholine by acetylcholinesterase is assumed to be a first order reaction. This assumption is accurate if inhibitors are not involved, which is true for normal synaptic physiology. This assumption ensures that our problem is linear and thus solvable.

The concentrations of acetylcholine are assumed to be of a magnitude large enough that diffusion can be looked at in a continuous manner. This is not ideal, due to the small number of neurotransmitter molecules released, but it was assumed to make the problem solvable within the scope of diffusion.

The concentration of acetylcholine with respect to time is simplified in the one dimension as follows:

$$\frac{\delta A_{(t,x)}}{\delta t} = D\frac{\delta^2 A_{(t,x)}}{\delta x^2} - kA_{(t,x)} \quad (10)$$

Where D is the diffusion coefficient of acetylcholine, and k is the rate of breaking down of acetylcholine by acetylcholinesterase.

2) Initial Conditions

The initial concentration of acetylcholine in the synaptic cleft is zero everywhere except at x=0, where a pulse of acetylcholine is released from the presynaptic vesicle, indicating the start of action potential. It is then diffused throughout the synaptic cleft. Mathematically, we can express this as:

$$A(x,0) = Ai\,\delta(x) \quad (11)$$

where A_i is the initial concentration of acetylcholine released and $\delta(x)$ is the Dirac delta function.

3) Boundary Conditions

At the presynaptic membrane, no reabsorption was assumed, resulting in a no flux boundary condition. Mathematically, this is expressed as:

$$\frac{\partial A}{\partial x} = 0|_{(t,x=0)} \quad (12)$$

At the postsynaptic membrane, acetylcholine is bound to ion channels, preventing it from contributing to the overall concentration in the cleft, and a Robin boundary condition is used.

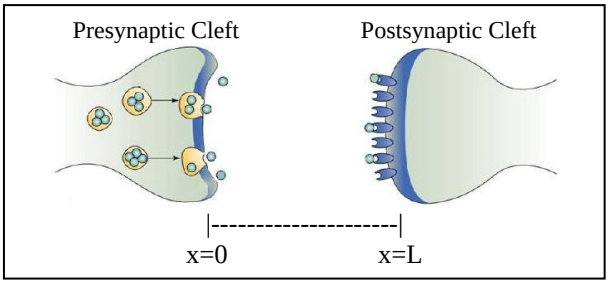

Fig. 2. Synaptic Cleft.[13]

$$-D\frac{\partial A}{\partial x}\Big|_{(t,x=L)} = A_{(x=L,t)} \quad (13)$$

The described system with activated enzyme in the complex geometry can be solved numerically to predict the concentration evolution of acetylcholine under normal neuromuscular operations.

The concentrations of acetylcholine are assumed to be of a magnitude large enough that diffusion can be looked at in a continuous manner. This is not ideal, due to the small number of neurotransmitter molecules released, but it was assumed to make the problem solvable within the scope of diffusion.

The concentration of acetylcholine with respect to time is simplified in the one dimension as follows: [14]

$$\frac{\delta A_{(t,x)}}{\delta t} = D\frac{\delta^2 A_{(t,x)}}{\delta x^2} - kA_{(t,x)} \quad (14)$$

TABLE III. NAMING CONVENTIONS OF INVOLVED COMPOUNDS

Symbol	Name
A	Acetylcholine
E	Acetylcholinesterase
AE	Michaelis Ligand-Substrate
acE	Acylate Enzyme
R	Unbound Receptor
A_2R	Single Bound Receptor
A_2R	Double Bound Closed Receptor
A_2R^{open}	Double Bound Open Receptor

IV. METHODOLOGY

Differential equations are solved using numerical methods to provide more accurate results. The more thorough the method, the more it can handle complex geometries and provide more accurate results. Mentioned below are four examples of numerical methods.

A. Finite Difference Method [8]

FDM involves discretizing continuous functions to approximate solutions to differential equations, especially when analytical solutions are challenging. By dividing the problem domain into a grid of discrete points, the method relies on the values of neighboring points to approximate the function. Its effectiveness is influenced by grid size and the order of the finite difference scheme employed.

B. Finite Element Method [8]

FEM is a numerical technique that divides a given domain into smaller, more manageable subdomains known as elements. These elements are interconnected at specific points referred to as nodes, forming a mesh structure. We can then solve the PDEs specified at the nodes of these elements. The choice of element size and shape is very flexible, so finite element methods can handle complex geometries, but requires a mesh generation process and many degrees of freedom to obtain accurate solutions.

C. Spectral Element Method [7]

The Spectral Element Method (SEM) uses advanced piecewise polynomial basis functions to expand the solution and thus achieves exceedingly high levels of accuracy. In SEM, the calculation error decreases exponentially as the order of the fitting polynomial increases, so rapid solution convergence to the exact solution is achieved even with fewer structural degrees of freedom compared to FEM. The main advantage of SEM is faster convergence speed. It also has lower numerical dispersion and requires fewer nodes per wavelength. Disadvantages of SEM include the difficulty in modeling complex geometries compared to the flexibility of FEM, so it is less widely used.

D. Runge-Kutta Method

The Runge-Kutta method is a single-step method that used a weighted average of several slopes to approximate the solution at each time step to determine the next point on the curve. It is based on the idea of approximating the solution curve by a series of short line segments, each of which is tangent to the curve at some point. It is more accurate and stable than the Euler method, which uses only one slope per interval. It can also handle nonlinear and stiff equations better than the Euler method.

In our process of modelling the Neuromuscular Junction, we decided to use and compare two methods which are: Finite Difference Method (FDM), and Finite Element Method (FEM).

E. Analytical Solution

To solve our problem analytically, the finite Fourier transform technique is applied to convert the PDE into a set of ODEs. Then, we solve an eigenvalue problem for the homogenous boundary conditions to find the unknown Fourier coefficients. Next, we use the orthonormality condition to evaluate the constant of integration. Finally, the Sturm-Liouville theory is employed to simplify the integration involving the basis functions and the PDE coefficients. [14]

$$A_{(t,x)} = \frac{2A_S}{L}\sum_{n=1}^{\infty}\sqrt{[1-\frac{1}{2\lambda_n}\sin(\lambda_n L)]}e^{-(D\lambda_n^2+k)t}\cos(\lambda_n x) \quad (15)$$

$$-\lambda_n \sin(\lambda_n L) + \frac{\beta}{D}\cos(\lambda_n L) = 0 \quad (16)$$

V. RESULTS AND ANALYSIS

A. Numerical Results

During our first modeling trials, we tried solving the equations and modelling the system using the Finite Difference method. Unfortunately, the FDM did not yield satisfying or conclusive results, as they were highly inaccurate and did not represent the NMJ's geometry clearly. We then opted for implementing the Finite Element method for the numerical solution.

The diffusion of acetylcholine across the synaptic cleft was modeled as a slab with the presynaptic neuron located at x=0 and the postsynaptic neuron at x=L (Figure 1). All

required constant values are listed in Table IV. The differential equation governing this problem is given as Equation (10), with initial condition given in Equation (11), and the boundary conditions given in Equations (12) and (13).

Equation (10) was solved in MATLAB using PDEPE function. The numerical partial differential equation solver solves equations in the form shown below:

$$c\left(x,t,u,\frac{\partial u}{\partial x}\right)\frac{\partial u}{\partial t} = \frac{\partial}{\partial x}\left(f\left(x,t,u,\frac{\partial u}{\partial x}\right)\right) + s\left(x,t,u,\frac{\partial u}{\partial x}\right) \quad (17)$$

To match Equation (10) to this form, c=1, f = $D\frac{\partial A}{\partial x}$, and s= -kA, where D is the diffusion coefficient of Ach, k is the rate constant of degradation of Ach by acetylcholinesterase. These coefficients were used in the subfunction pdex1pe to define the PDE.

MATLAB PDE toolbox provides a user interface to numerically solve PDEs using FEA. FEA involves creating a mesh of triangles based on the defined geometry and approximating the PDE solution as a system of ordinary differential equations at each node of the mesh. The geometry generated for our simulation (Figure 3), contains a vesicle fusing to the presynaptic membrane (left side), the post synaptic membrane (right side), and the edges of the synaptic cleft (top and bottom).

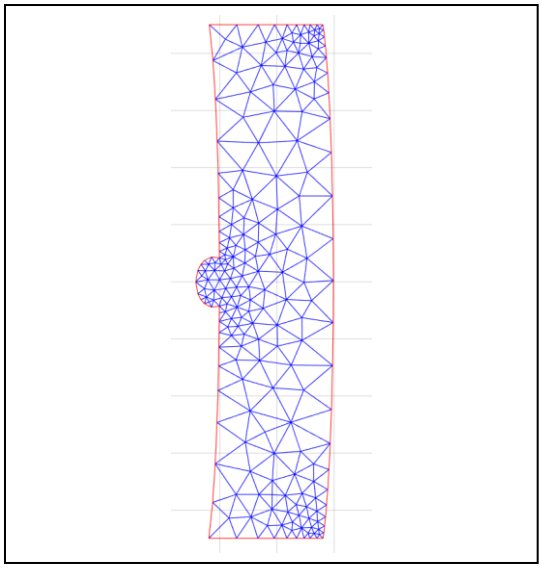

Fig. 3. Finite Element Method Geometry and Mesh

In the case of Myasthenia Gravis, it was found that the rate of degradation of acetylcholine receptors increased two or three folds. This drastic decrease in the number of acetylcholine receptors results in fewer interactions between acetylcholine and its receptors, leading to decreased activation of action potentials.[14] In our simulation, we decreased the flux of acetylcholine by a factor to represent the change of its binding to its receptors.

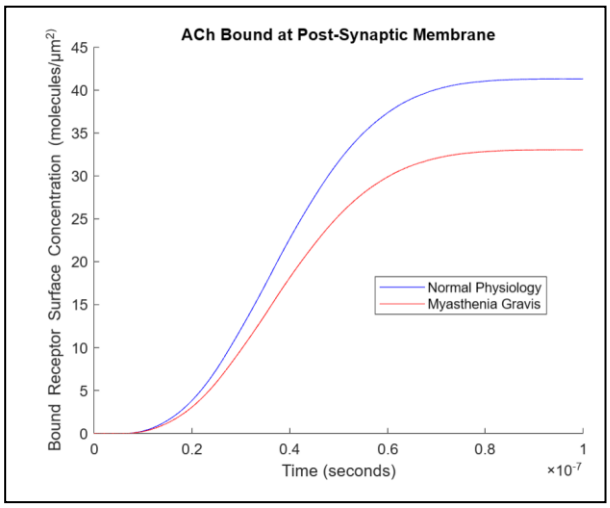

Fig. 4. Number of bound ACh molecules with respect to time.

The y-axis quantifies the amount of acetylcholine molecules bound to the receptors on the postsynaptic membrane surface area (Figure 4). A higher value on the y-axis indicates more acetylcholine molecules are bound to the receptors, implying a stronger signal transmission across the synapse. Since the number of receptors is limited, the curve goes into a steady state after some time. In MG, the curve goes into the steady state at a lower concentration and at a higher rate than in normal cases, which indicates the increase in the rate of breaking down of acetylcholine by acetylcholinesterase.

To model the sudden release of acetylcholine in the presynaptic vesicle, an if statement is used in place of the delta function, which is not present in MATLAB.

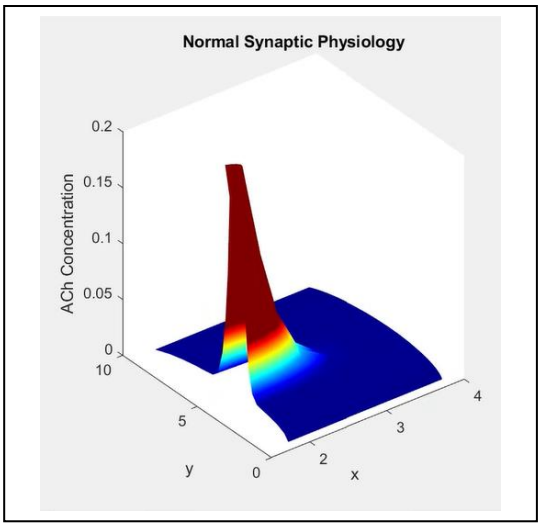

Fig. 5. Concentration of ACh at the the start of action potential.

The initial concentration of acetylcholine is set to be high inside the merging vesicle and zero elsewhere (Figure 5). For the simulation of both the normal synaptic physiology and Myasthenia Gravis, a consumption term was introduced to represent the effects of acetylcholinesterase breaking down acetylcholine. In the case of MG (Figure 8), the consumption term used was of a higher value than in the normal case, to represent the increase in the rate of degradation of acetylcholine by the enzyme.

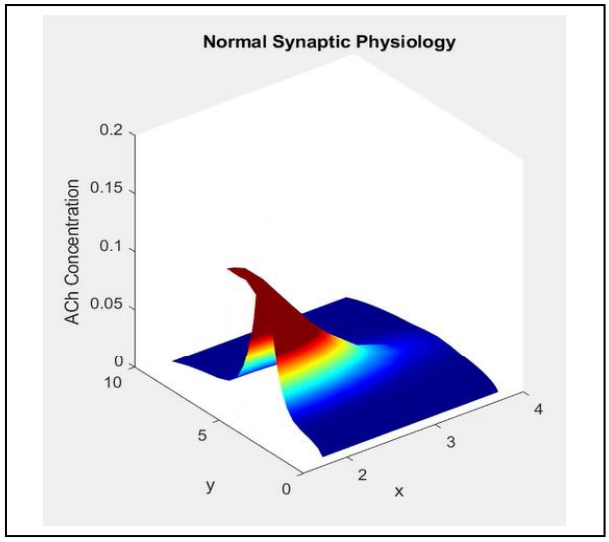

Fig. 6. Diffusion of acetylcholine through the synaptic cleft over time.

The high concentration of acetylcholine can be seen diffusing throughout the synaptic cleft from the presynaptic vesicle during the action potential (Figure 6).

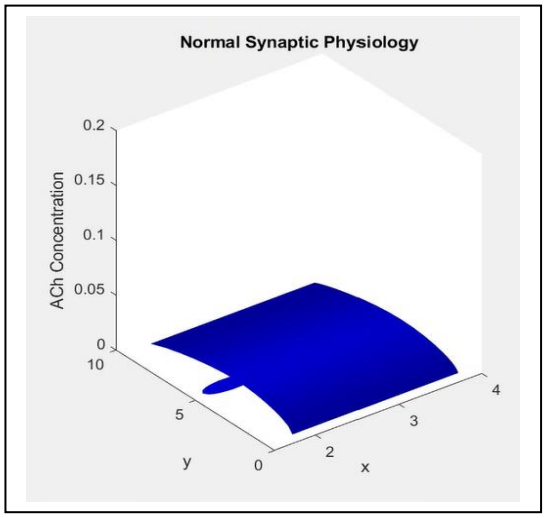

Fig. 7. Concentration of ACh at the end of action Potential.

After the action potential, the concentration of acetylcholine remains constant through the cleft and the presynaptic vesicle for a short amount of time before the start of the next action potential (Figure 7). In the case of MG, this state is reached faster than in normal synaptic physiology, due to the quicker degradation of the neurotransmitter by acetylcholinesterase enzyme.

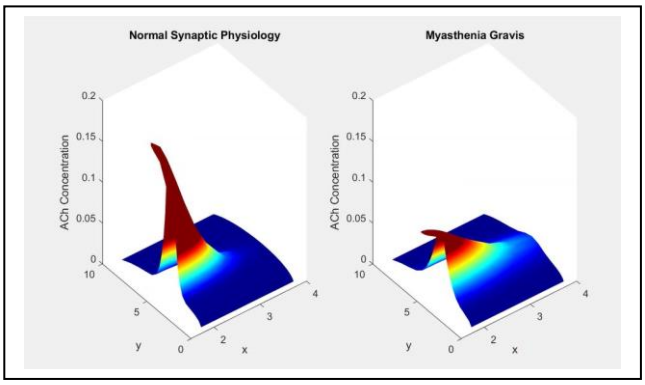

Fig 8. Change in concentration of acetylcholine in the synaptic cleft in normal case vs. Myasthenia Gravis case at the same time point

In the case of Myasthenia Gravis, the rate of degradation of acetylcholine in the synaptic cleft is higher. In our MATLAB code, this can be represented by introducing new terms *mg_a* and *mg_c* to represent the rate of breakdown of the neurotransmitter and the rate of its diffusion away from the cleft respectively. The values of *mg_a* and *mg_c* are higher than normal case which is represented by terms *a* and *c*. We can see that the concentration of acetylcholine in the synaptic cleft decreases at a faster rate in the case of Myasthenia Gravis compared to normal cases (Figure 8).

TABLE IV. VALUES FOR CONSTANTS USED IN SIMULATION

Variable	Description	Value
D	Diffusion Coefficient of Ach	400 m^2
L	Synaptic Cleft Distance	20 nm
k	ACh Degradation Rate	2333 s^{-1}
β	ACh Receptor Binding Rate	4.7E7 $M^{-1}s^{-1}$
A_i	Initial Ach Released	0.006 mmol/m^2
Synapse Shape	-	r = 150nm L= 20nm

VI. CONCLUSION AND FUTURE WORK

Our model successfully utilized the finite element method to visualize the effect of Myasthenia Gravis on the neuromuscular junction with high accuracy, we achieved the high accuracy by trying different methods like finite difference method and finite element method.

Our investigation into solving the problem using both the finite difference method (FDM) and the finite element method (FEM) has revealed conflicting outcomes. While the FDM did not yield satisfactory results, the FEM proved to be effective in providing us the high accuracy with short time needed of calculations.

Future work can involve further validation and optimization of the model, integration of additional features, and using more complex methods, like the spectral element method (SEM) to achieve even higher accuracy and precision. With such higher accuracy, we can hopefully aid doctors and researchers in the medical field in understanding Myasthenia Gravis better, which might help them finally find a cure.

Overall, this research demonstrates the potential for advancements in describing and visualizing neuromuscular disorders using the finite element method and can be further enhanced using a more accurate method.

ACKNOWLEDGMENTS

This study is submitted for the course Special Functions and Partial Differential equations (MTH2245), and was done under the supervision of Dr. Samah El Shafiey, PhD associate professor, Engineering Mathematics and Physics Department at Cairo University, Faculty of Engineering.

REFERENCES

[1] Mayo Clinic. (2021). Myasthenia gravis - Symptoms and Causes.

[2] Howard JF. Clinical overview of MG. Myasthenia Gravis Foundation of America. (Accessed February 7, 2022).

[3] Peragallo JH, Bitrian E, Kupersmith MJ, et al. Relationship between age, gender, and race in patients presenting with myasthenia gravis with only ocular manifestations. J Neuroophthalmol. (2016)

[4] Prevalence of neuromuscular disorders in Qena governorate/Egypt: population-based survey - PubMed (nih.gov)

[5] Smart JL, McCammon JA. Analysis of synaptic transmission in the neuromuscular junction using a continuum finite element model. Biophys J. 1998 Oct;75(4):1679-88.

[6] Khaliq, A., Jenkins, F., DeCoster, M., & Ali, M. (2011). A new 3D mass diffusion–reaction model in the neuromuscular junction. Journal of Computational Neuroscience, 30(4), 729-745

[7] Liu D, Wang Y, DeCoster MA. (2013). Spectral Element Simulation of Reaction-Diffusion System in the Neuromuscular Junction. Journal of Applied & Computational Mathematics, 2(4), 136. doi:10.4172/2168-9679.1000136

[8] Springer Handbook of Materials Measurement Methods, Finite Element and Finite Difference Methods

[9] Naka, T., & Shiba, K. S. (1997). A two-dimensional compartment model for the reaction diffusion system of acetylcholine in the synaptic cleft at the neuromuscular junction. Biosystems, 41, 17–27.

[10] Wathey, J. C., & Nass, M. N. (1979). Numerical reconstruction of the quantal event at nicotinic synapses. Biophysical Journal, 27, 145–164.

[11] Bird, S.J. (7 August 2023) Overview of the Treatment of Myasthenia Gravis, UpToDate.

[12] P. Schatz, "Biology," Phil Schatz, 2021. Available at: https://philschatz.com/biology-book/contents/m44451.html.

[13] R. Kimura, “Myasthenia Gravis,” The Brain from Top to Bottom, 2002. Available at: https://thebrain.mcgill.ca/flash/capsules/pdf_articles/myasthenia.pdf.

[14] Hagan, T. et al. (2010) Diffusion of acetylcholine in the synaptic cleft. Available at: https://isn.ucsd.edu/courses/Beng221/problems/2010/project1.pdf

APPENDIX: MATLAB CODE

A. PDE toolbox to initiate parameters

```
% This script is written and read by
pdetool and should NOT be edited.
% There are two recommended alternatives:
% 1) Export the required variables from
pdetool and create a MATLAB script
%    to perform operations on these.
% 2) Define the problem completely using a
MATLAB script. See
%
https://www.mathworks.com/help/pde/example
s.html for examples
%    of this approach.
function pdemodel
[pde_fig,ax]=pdeinit;
pdetool('appl_cb',10);
set(ax,'DataAspectRatio',[10 10 1]);
set(ax,'PlotBoxAspectRatio',[1 1 2]);
set(ax,'XLim',[0 10]);
set(ax,'YLim',[0 10]);
set(ax,'XTick',[
0,1,2,3,4,5,6,7,8,9,10,]);
set(ax,'YTick',[
0,1,2,3,4,5,6,7,8,9,10,]);
pdetool('gridon','on');

% Geometry description:
pdeellip(1.7056396148555697,5.030949105914
7193,0.29573590096286106,4.879642365887207
2,0,'E1');
pdeellip(3.6960110041265466,4.989683631361
7605,0.29573590096286106,4.879642365887207
2,0,'E2');
pderect([1.7400275103163696
3.7070151306740033 9.745529573590094
0.33700137551581744],'R1');
pderect([4.2434662998624484
1.4099037138927111 9.4979367262723517
9.9518569463548818],'R2');
pderect([3.9546079779917465
1.5199449793672624 0.068775790921597135
0.50206327372764825],'R3');
pdeellip(1.9050894085281982,4.989683631361
7614,0.31636863823933936,0.443603851444291
49,...
0,'E3');
set(findobj(get(pde_fig,'Children'),'Tag',
'PDEEval'),'String','R1-E1-R2-R3+E2-R2-
R3+E3')

% Boundary conditions:
pdetool('changemode',0)
pdetool('removeb',[1 2 10 14 15 18 19 ]);
pdesetbd(14,'neu',1,'0','0')
pdesetbd(13,'neu',1,'0','0')
pdesetbd(12,'neu',1,'0','0')
pdesetbd(11,'neu',1,'0','0')
pdesetbd(10,'neu',1,'1','0')
pdesetbd(9,'neu',1,'1','0')
pdesetbd(8,'neu',1,'0','0')
pdesetbd(7,'neu',1,'0','0')
pdesetbd(6,'neu',1,'0','0')
pdesetbd(5,'neu',1,'0','0')
pdesetbd(4,'neu',1,'0','0')
pdesetbd(3,'neu',1,'0','0')
pdesetbd(2,'neu',1,'0','0')
pdesetbd(1,'neu',1,'0','0')

% Mesh generation:
setappdata(pde_fig,'Hgrad',1.3);
setappdata(pde_fig,'refinemethod','regular
');
setappdata(pde_fig,'jiggle',char('on','mea
n',''));
setappdata(pde_fig,'MesherVersion','preR20
13a');
pdetool('initmesh')

% PDE coefficients:
pdeseteq(2,'4000','0.0','0','1.0','0:100',
'0','0.0','[0 100]')
setappdata(pde_fig,'currparam',['1.0';'1.0
'])

% Solve parameters:
setappdata(pde_fig,'solveparam',char('0','
1000','10','pdeadworst','0.5','longest','0
','1E-4','','fixed','Inf'))

% Plotflags and user data strings:
setappdata(pde_fig,'plotflags',[1 1 1 1 1
1 1 1 0 0 0 1 1 0 0 0 0 1]);
setappdata(pde_fig,'colstring','');
setappdata(pde_fig,'arrowstring','');
setappdata(pde_fig,'deformstring','');
setappdata(pde_fig,'heightstring','');
```

B. Plotting 2-D graph of concentrations

```
function boundReceptors
%Parameters
L=0.02; %µm
tfinal=1e-7; %seconds
D=400; %µm^2/s
tpoints=501;
xpoints=41;
%m=0 denotes that our problem is in a slab
m = 0;
%Create time and distance vectors
x = linspace(0,L,xpoints);
t = linspace(0,tfinal,tpoints);
%Call pdepe to solve the equation
sol =
pdepe(m,@pdex1pde,@pdex1ic,@pdex1bc,x,t);
%Solution is first component of sol
C = sol(:,:,1);
%Estimating flux at boundary
Flux=zeros(1,length(t));
for i=2:501
```

```
dFlux=-D*((C(i,41)-
C(i,40))/(L/xpoints))*(tfinal/tpoints);
Flux(i)=Flux(i-1)+dFlux;
end
%Plotting Flux vs time
% Plot both curves on the same figure
figure
hold on;
plot(t, Flux*6.022e23, 'b');
plot(t, 0.8*Flux*6.022e23, 'r');
hold off;
xlabel('Time (seconds)');
ylabel('Bound Receptor Surface
Concentration (molecules/µm^2)');
title('ACh Bound at Post-Synaptic
Membrane');
legend({'Normal Physiology', 'Myasthenia
Gravis'},'Location','best');
%PDE function (define our PDE)
function [c,f,s] = pdex1pde(x,t,Conc,DCDx)
D=400; %µm^2/s
k=23e7; %1/s, kcat of AChE
%Time derivative coefficient
c = 1;
%x derivative coefficient (includes first
derivative to make a second
%derivative in x)
f = D*DCDx;
%Forcing function coefficient
G=-k*Conc; %mol/µm^3 s
s = G;
%IC function
function C0 = pdex1ic(x)
Cs=6e-13; %mol/µm^2,
concentration pulse into synapse
%Delta function initial condition,
concentration is Cs at x=0 and 0
%elsewhere
if x==0
 C0=Cs;
else
 C0=0;
end
%BC function
function [pl,ql,pr,qr] =
pdex1bc(xl,ul,xr,ur,t)
beta=4.77e22; %µm^3/mol*s Receptor binding
rate
%dCdX=0 at x=0
pl = 0;
ql = 1;
%-beta*Conc-D*dCdx=0 at x=L (Robin BC)
pr = -beta*ur;
qr = -1;
```

C. 3-D plot of Normal case vs Myasthenia Gravis

```
% Load SynapseModel.m in pdetool and
export the parameters
% Must export the variables b, p, e, t, c,
a, f, d from pdetool
clf
% Determine length of simulation and time
step
tlist = 0:0.01:0.5;
% Define initial conditions
u0 = zeros(size(p, 2), 1); % Set
everything to zero
n = 11; % Number of nodes the initial
concentration is spread over
Cs = 10; % Initial concentration
set = [181, 141, 140, 175, 105, 133, 176,
139, 104, 180, 138]; % Data points in
vesicle
for i = 1:size(set, 2)
    u0(set(i)) = Cs / n;
end

% Define global sink term due to cleavage
in the cleft for different conditions
a1 = '0';
a2 = '5';
c = '10';

% Define parameters specific to myasthenia
gravis (MG)
mg_a = '5'; % Adjust this value based on
the impact of MG on the sink term 'a'
mg_c = '25'; % Adjust this value based on
the impact of MG on the sink term 'c'
% Solve PDE for normal condition and Sarin
gas condition
u1 = parabolic(u0, tlist, b, p, e, t, c,
a1, f, d);
u2 = parabolic(u0, tlist, b, p, e, t, c,
a2, f, d);

% Solve PDE for MG condition
u_mg = parabolic(u0, tlist, b, p, e, t,
mg_c, mg_a, f, d);

% Run multiple iterations for normal,
Sarin gas, and MG conditions
for i = 1:3
    ui1 = u0 + u1(:, end);
    ui2 = u0 + u2(:, end);
    ui_mg = u0 + u_mg(:, end);

    uf1 = parabolic(ui1, tlist, b, p, e,
t, c, a1, f, d);
    uf2 = parabolic(ui2, tlist, b, p, e,
t, c, a2, f, d);
    uf_mg = parabolic(ui_mg, tlist, b, p,
e, t, mg_c, mg_a, f, d);

    u1 = [u1, uf1];
    u2 = [u2, uf2];
    u_mg = [u_mg, uf_mg];
end
```

```
clear M
for j = 1:size(u1, 2)

    subplot(1, 2, 1)
    pdesurf(p, t, u2(:, j))
    xlabel('x')
    ylabel('y')
    zlabel('ACh Concentration')
    title('Normal Synaptic Physiology')
    colormap('jet')
    caxis([0 .05])
    axis([1.5 4 0 10 0 .2])

    subplot(1, 2, 2)
    pdesurf(p, t, u_mg(:, j))
    xlabel('x')
    ylabel('y')
    zlabel('ACh Concentration')
    title('Myasthenia Gravis')
    colormap('jet')
    caxis([0 .05])
    axis([1.5 4 0 10 0 .2])

    % Calculate time in milliseconds for
the current step
    % current_time_ms = tlist(j) * 1000;
    % Add a title with the current time
step in milliseconds
    % sgtitle(['Time: ',
num2str(current_time_ms), ' ms'])
    M(j) = getframe(figure(1));
end

movie2avi(M, 'moviecompressed',
'compression', 'Cinepak')
```